Performance Analysis of a Handheld Aspiration-Assisted Device for End-Cut Prostate Biopsy

Ungurait, Dane[1]
University of Florida
483 Wertheim Lab, Gainesville, FL 32611
daungurait97@ufl.edu
ASME Member

Araya, Roy
University of Florida
43 Florence St, Malden, MA, 02148
royaraya16@gmail.com

Brisbane, Wayne
University of California – Los Angeles
757 Westwood Plaza, Los Angeles, CA 90095
wbrisbane@mednet.ucla.edu

Lampotang, Samsun
University of Florida
Box 100254, 1600 Archer Road, Gainesville, FL 32610
slampotang@anest.ufl.edu

Lawrence, Elisabeth
Hamilton College
1062 E Lancaster Ave, Bryn Mawr, PA 19010
bess.lawrence@gmail.com

Yamaguchi, Hitomi
University of Florida
483 Wertheim Lab, Gainesville, FL 32611
hitomiy@ufl.edu
ASME Fellow

[1] Corresponding author information can be added as a footnote.

ABSTRACT

Needle biopsy is a common procedure used to diagnose various types of cancer, particularly prostate cancer. Current needle biopsy devices used in this procedure feature End-Cut and Side-Cut needles. They also typically have a loud and sudden spring-loaded firing mechanism with inaccurate needle positioning that can cause additional harm to the patient. A novel aspiration-assisted biopsy device has been developed by researchers at the University of Florida that uses a coaxial End-Cut needle attached to a syringe. The device utilizes vacuum pressure to retain tissue during the biopsy procedure and does not have a spring-loaded firing mechanism. This paper describes the design and development of the device and characterizes its performance by testing it on animal tissue ex-vivo alongside two other commercial biopsy devices currently used in clinical settings. Tests performed on bovine cardiac tissue ex-vivo indicated that the developed device performs comparably to the two commercial biopsy devices.

INTRODUCTION

Prostate cancer is a deadly disease caused by the unregulated growth and reproduction of cells in the prostate, a reproductive organ found in individuals with male anatomy. It is estimated that approximately 1 in 8 males will be diagnosed with prostate cancer within their lifetime, and 1 in 41 males will pass away from this disease [1]. Fortunately, the death rate from this disease has been declining in recent years, largely due to improvements in diagnostic technologies as early detection of the disease is strongly correlated with successful cancer treatment. Comparison of the survival rates of cancer patients diagnosed across the 4 stages of cancer (I through IV) has shown that patients diagnosed in the earlier stages of cancer (I and II) have more than double the 5-year survival rate than patients diagnosed in the later stages (III and IV) [2]. Further

improvements to diagnostic practices and technologies can further improve the detection rate of patients with prostate cancer.

Most prostate biopsy devices are core needle biopsy devices, which use a needle to cut through tissue and then store the sample in a hollow section of the needle. Their widespread use can primarily be attributed to their ease of use [3]. Core needle biopsy devices can be further divided into two needle types: Side-Cut (also called Tru-Cut) needles and End-Cut needles. Table 1 lists several commercially available prostate biopsy devices along with several key features of the devices, including needle type and size.

Side-Cut needle biopsy devices are widely used in clinical settings today. Side-Cut needles feature a solid needle with a notch cut into the side of the needle. They also feature an outer cannula that fires (usually spring-loaded) and slides over the needle to cut through surrounding tissue and retain tissue inside the notch of the inner needle. Commercial Side-Cut needle biopsy devices include the Max-Core, Magnum, and Monopty made by Bard; the Temno, and the Achieve made by Merit Medical; and the SuperCore, and Tru Core made by Argon Medical Devices.

There are several inherent limitations and disadvantages to Side-Cut needle biopsy devices as shown in Fig. 1. The first is that the size of the collected sample is limited by the size of the notch in the needle (Fig. 1a). Current biopsy devices also lack the ability to indicate the orientation of the sample once it is removed and deposited in a receptacle (Fig. 1b). Each device model can only collect one target sample length, and the thickness of the sample must be smaller than the diameter of the needle. This can

result in the need for multiple cores to collect an adequate sample (Fig. 1c). Side-Cut needles can also bend at the notch due to the thinner material at that section (Fig. 1d). This bending can lead to inaccurate needle positioning. Since the notch in the needle cannot be located at the end of the needle, Side-Cut needles also damage tissue located behind the sampling region (Fig. 1e). Another common issue associated with these devices is that the high speed of the spring-loaded firing mechanism can cause patient discomfort even when local anesthesia is applied (Fig. 1f). Despite these limitations, Side-Cut needles are still the most prevalent biopsy needles used today for prostate cancer biopsies.

End-Cut needles use a coaxial needle featuring a solid stylette for penetration and rigidity along with an outer cannula that slides over the stylette during operation. Tissue is stored inside the outer cannula of the coaxial needle, and pushed out of the canula using the stylette after the sample has been collected. The use of a hollow needle instead of a notch allows for a larger sample collection volume, but tissue retention methods vary between these devices, and they are not always very effective. A study in 1995 found that End-Cut needles could have zero biopsies (biopsy cores that yield no tissue) at a rate of up to 73% depending on several factors such as type of tissue and needle diameter [13]. Tissue retention methods have improved since this study, leading to a rise in their popularity; however, the Side-Cut needle is still more prevalent. Like their Side-Cut needle counterparts, they typically use a spring-loaded firing mechanism that can startle the patient and cause discomfort. One such End-Cut needle biopsy device (BioPince made by Argon Medical) collects a full core sample using a

triaxial needle with three components: a solid inner stylette, a hollow outer cannula with a slit cut at the distal end, and an outer pincer that slides into the slit at the end of the operation to help cut through and hold the stored tissue inside the needle. Other examples of commercial End-Cut needle biopsy devices include the CorVocet by Merit Medical, and the MorCor by Hatch Medical.

A study in 2017 demonstrated the development of an aspiration-assisted biopsy device [14]. The device utilizes an End-Cut, coaxial needle to collect and extract large volume samples with minimum tissue distortion. The original proof-of-concept build used a large linear stage to move the syringe and needle components; however, this design was too large and impractical for clinical use. A smaller, more ergonomic handheld prototype of the device was developed using a DC motor and a lead screw to induce the linear motion of the syringe and needle components. This paper will describe phantom tissue properties considered when testing prostate biopsy devices. It will then explain the design and development of the handheld prototype biopsy device. Finally, the device will be characterized by comparing its performance with two biopsy devices that are currently on the market.

MECHANICAL PROPERTIES OF PROSTATE TISSUE

The measured mechanical properties of biological tissues are highly dependent on the methods used to obtain them. This can be attributed to the complex nature of biological tissues, which are responsive to their environment and unique to each individual.

The stiffness of prostate tissue not only can affect biopsy performance, but also plays a large role in cancer metastasis. Cells that are less stiff can be more easily compressed and slip through the basal lamina of the endothelium and enter the bloodstream [15]. This means cancer cells that are less stiff are more likely to metastasize. This shows that the stiffness of prostate tissue can potentially be used to diagnose cancer.

When the stiffnesses of benign prostate hyperplasia tissue (BPH) and cancerous prostate tissue are compared to each other, a seemingly contradictory set of trends emerges: cancerous tissues have larger Young's moduli at the macroscopic (bulk) scale compared to BPH, but smaller Young's moduli at the microscopic (cellular) scale. This trend has been analyzed using transrectal real-time tissue elastography (RTE) for bulk prostate tissue, and atomic force microscopy (AFM) for prostate cells [16]. The RTE testing yielded average strain indexes of 4.81 (standard deviation of 6.15) and 25.64 (standard deviation of 10.16) for BPH and cancerous tissue respectively. Testing using shear wave elastography (SWE) has also been done and further supports the finding that bulk BPH tissue (17.5 ± 2.5 kPa) is less stiff than bulk cancerous prostate tissue (90.5 ± 4.5 kPa) [17]. AFM testing yielded average Young's moduli of 3.03 kPa (standard deviation of 0.64 kPa) and 1.72 kPa (standard deviation of 1.22 kPa) for BPH cells and cancerous prostate cells respectively [16].

It is believed that cancerous prostate cells are less stiff than their healthier counterparts due to increased expression of matrix metalloproteinase-2 (MMP-2) and reduced expression of collagen [16]. MMP-2 is capable of degrading collagen, and

collagen is known to play a key role in cellular stiffness. At the macroscopic scale, cancerous prostate tissue is believed to be stiffer due to the rapid growth and replication of the cells in a confined space. This rapid growth in a small space results in the compression of the tissue, which increases the bulk stiffness of the tissue, even though the individual cells are less stiff on their own.

When needle biopsy devices are tested on phantom materials, it is important that the phantom materials behave similarly to the tissue that the device is intended to collect. This means that the phantom materials should possess similar mechanical properties to both healthy and cancerous prostate tissue. The bulk tissue stiffnesses of the phantoms used to test the biopsy devices in this paper were greater than or equal to the lowest reported stiffness of healthy tissue (15 kPa), and less than or equal to the highest reported stiffness of cancerous tissue (95 kPa) [17].

TISSUE COLLECTION EFFECTIVENESS OF HANDHELD ASPIRATION-ASSISTED BIOPSY DEVICE

Handheld Aspiration-Assisted Biopsy Device Design

A schematic illustrating the sample collection sequence for the developed device (hereafter called the *UF device*) is shown in Fig. 2. The UF device consists of a syringe with a coaxial needle featuring a solid inner stylette connected to the syringe plunger, and a two-pronged external needle attached to the syringe barrel via a Luer Lok connection. The needle is first inserted into the tissue until it reaches the desired tissue sampling region. Next, the plunger and stylette remain stationary inside the device's housing while the syringe barrel and external needle advance forward. This motion is

driven by a direct current (DC) motor and a lead screw with a 3D printed threaded lead nut that connects the syringe barrel to the lead screw. Once the lead nut finishes traveling along the length of the lead screw and begins to jam against the coupler, the current flowing through the DC motor spikes to the stall current value. This current spike is detected by a current sensor in the device and serves as a signal to cut off power to the motor until a button is pressed to move the motor back in the opposite direction. This control mechanism allows for the throw length of the device to be controlled by changing the thickness of the lead nut. Once the motor stops running, the device is manually retracted from the sample tissue. The vacuum from the relative motion of the syringe and needle components holds the collected tissue inside of the external needle while the device is retracted, and the sample breaks off in tension. Once the device is removed from the sample tissue, the collected sample can be extracted by actuating the motor, or by removing the syringe from the device and manually pushing the syringe plunger to expel the tissue from the needle.

The plastic housing for the handheld aspiration-assisted biopsy device was designed to comfortably fit in the user's hand and to minimize user strain during operation. An overview of the main components housed inside the device are shown in Fig. 3. The housing was 3D printed out of polylactic acid (PLA) to allow for easy rapid fabrication as well as to minimize product weight. The overall dimensions of the full assembly (excluding the needle) were approximately 158 mm long, 42 mm wide, and 58 mm deep. The housing is shaped like an ellipsoid with a groove pattern on the bottom surface for the user's fingers to rest in. These grooves are 2.5 mm deep and 25 mm

apart. These dimensions were selected to accommodate the 5th and 95th percentile index finger breadth and thickness measurements of male and female hands based on anthropometric hand data that was compiled from military and civilian sources in 1996 [18]. The device was designed with the intent that it would be held using a power grip with the user's thumb along the length of the device to provide additional precision with manipulation of the device. With this grip in mind, it is recommended that the diameter of the handle be kept under 50 mm to ensure adequate grip across a large range of hand sizes [19]. Due to difficulties accommodating the various internal components, the smallest achievable maximum diameter of the device was 58 mm.

Inside the housing, there is a wall in the middle with a circular groove for a 20 mL plastic syringe to snap into place. This wall also had mounting holes to mount a 20 mm diameter gearmotor. On the bottom of the housing towards the proximal end and away from the finger grooves, there was a hole for the motor wires to pass through to be connected to an external controller circuit. On the proximal side of the housing, there were two circular holes: one for the syringe plunger flange to snap into place, and one for a lead screw to rest inside. On the distal side of the housing and cover, there was a small circular cut-out for an 18-gage needle to fit through.

To actuate the syringe and needle components, a 6 V DC 20 mm diameter gearmotor and a brass lead screw with a diameter of 3 mm and a pitch of 2.5 mm were used. The motor was mounted to a wall inside the housing using M2.5 screws. The motor was coupled to the lead screw using a custom 3D printed PLA coupler and a metal pin. The lead screw rested inside a shallow hole on the proximal end of the housing. A

custom threaded, 3D printed lead nut was printed out of PLA to travel along the lead screw. The lead nut had a circular hole for the syringe barrel to snap into place, and a notch for the syringe barrel flange to fit into.

To control the device and allow for a customizable throw length, an external controller circuit was used. Fig. 4 shows the device alongside the controller circuit, with labeled components. The circuit was built using a breadboard external to the device and connected to the motor via a wire that passed through a hole on the bottom surface of the housing. The circuit featured a 9 V battery, an ON/OFF switch, a light emitting diode (LED), a motor driver, a current sensor, a push button switch, several resistors, the 6 V DC gearmotor, and an Arduino UNO. The Arduino UNO served as the controller for the device and was wired to the push button, the current sensor, and the motor driver. Pushing the button would signal to the Arduino UNO to begin sample collection or sample extraction depending on the device state (whether a sample has been collected yet). The Arduino UNO would then send signals to the motor driver to control the speed and direction of the motor shaft's rotation. The direction of rotation depended on whether the device was in the collection or extraction stage. The device was configured to always run at full speed. The Arduino UNO was wired to the current sensor to receive readings of the current passing through the motor. When the device reaches the end of the collection and extraction stages, the lead nut begins to jam into the housing. This jamming causes the current to spike as the motor attempts to overcome this resistance. The Arduino UNO was programmed to stop the motor's motion and transition into a standby state when the current reading exceeded a specified stall current value. The

Arduino UNO would then send signals to the motor driver to initiate motor motion once the push button was pressed again. The LED in the circuit was wired in series to the ON/OFF switch and the 9 V battery to indicate when the circuit was powered on. A higher voltage battery was used due to concerns that the additional circuit components may draw too much power away from the motor. There were already power issues with a previous version of this device, so the battery voltage was increased from 6 V to 9 V to alleviate this concern. The voltage was higher than what the DC gear motor was rated for, so it is possible that the motor's lifespan may deteriorate in the future from this change, but no damage or motor performance issues have been observed yet since making this change. The batteries were not rechargeable.

To ensure the motor was capable of providing enough power to actuate the device, modifications were made to the syringe. A plastic disposable syringe barrel with an internal diameter of 20 mm was used with a plunger and rubber seal originally designed for a disposable 20 mL Becton Dickinson syringe (model 302830) with an internal barrel diameter of 19 mm. This decreased the interference between the seal and the barrel walls, which weakened the vacuum but also reduced the friction between the seal and the barrel. This decrease in vacuum strength was too large, so 1.5 turns of polytetrafluoroethylene (PTFE) sealant tape (thickness: 0.102 mm) was wrapped around the seal of the plunger to slightly increase the interference and vacuum strength. These changes resulted in a net decrease in the vacuum strength of the syringe as well as the friction within the device. It made it easier for the motor to move the syringe barrel and external needle, while also maintaining enough vacuum to collect and retain tissue.

Figure 5 shows the modified needle components and the final modified needle-syringe assembly.

The inner stylette had a diameter of 0.94 mm, was made of 304 stainless steel, and was attached to the syringe plunger. An 18-gage (1.27 mm OD, 1.14 mm ID), two-pronged, U-shape tip needle made from 316 stainless steel capillary tubing was attached to the barrel of the syringe via a Luer Lok connection. The external needle was about 100 mm long, and the inner stylette tip extended just past the tips of the external needle when the syringe and coaxial needle was fully assembled. The device was designed such that the syringe and needle components can easily be replaced, allowing the device to be reusable.

Tissue Collection Testing Methodology

The performance of the UF device was tested on six different animal tissues (ovine kidney, porcine kidney, porcine liver, bovine kidney, bovine liver, and bovine cardiac tissue) acquired from a local grocery store along with two different concentrations of gelatin (7 g per 100 mL of deionized water and 21 g per 100 mL of deionized water). The Young's moduli of the two gelatin samples were previously measured via compression testing and were 18 ± 1 kPa and 31 ± 1 kPa for the low and high concentrations, respectively. The performance of the UF device was also compared with two commercial devices. The BioPince (Argon Medical) uses a spring-loaded firing mechanism to move the needle components and collect tissue. The total length of the exposed needle is 230 mm. For this experiment, the throw length was set to 33 mm for every trial. The Max-Core is one of many models of Side-Cut needle biopsy devices made

by Bard. For this experiment, the 18-gage version (model 1825) was used to maintain a constant needle size with the UF device and BioPince. The maximum length of the exposed needle is 255 mm. Unlike the UF device and the BioPince, the Max-Core 1825 does not allow for a customizable throw length or core length. The only throw length that the 1825 model can be set to is 22 mm, and the needle notch length (core length) is 18 mm. Like the BioPince and many other Side-Cut needle biopsy devices, the 1825 model uses a spring-loaded firing mechanism to actuate the needle components.

Figure 6 shows the 3 biopsy devices that were tested, and Table 2 summarizes and compares the core features of the 3 devices. Figure 7a illustrates the aspiration-assisted biopsy device needle insertion for collection of a sample of low concentration gelatin. Figure 7b shows the bovine cardiac tissue that was used to test the biopsy devices.

As mentioned previously, the UF device is an aspiration-assisted biopsy device that features a coaxial End-Cut needle attached to a modified 20 mL syringe. The syringe is operated using a lead screw driven by a DC motor powered by a 9 V battery. Although the throw length of the device is not currently programmable, the throw length can be controlled by changing the thickness of the 3D-printed lead nut carrying the syringe. For this experiment, a nut was printed to set the throw length to 33 mm so that it matched the maximum throw length of the BioPince device that was used during testing. The device could detect when the motor was stalling via the current sensor. The device was configured so that the motor would stop running and prepare to switch directions once the motor current exceeded 900 mA.

The samples collected from these trials then had their lengths and masses measured and recorded. The results were then analyzed by a physician with experience performing prostate needle biopsies in a clinical setting to select the type of phantom tissue that was most comparable to human prostate tissue based on his professional experience. Next, twelve sequential trials were performed with each biopsy device on the selected tissue and the sample lengths and masses were recorded to analyze and compare performance.

Tissue Collection Testing Results

A summary of the lengths and masses of the samples collected from each of the phantom materials is presented in Fig. 8. These trials showed that the UF device collected longer and more massive samples than either of the commercial devices that are used to perform prostate biopsies for several tissues, most notably the low concentration gelatin and the cow liver sample. This may indicate that that the UF device is effective at collecting a wider range of tissue types and may have applications beyond prostate tissue biopsy.

Once bovine cardiac tissue was selected as the most comparable to human prostate tissue among the animal tissues tested, 12 additional samples were collected using each of the three biopsy devices. Figure 9 shows representative images of the bovine cardiac tissue samples that were collected using each of the three devices, while Fig. 10 summarizes the average lengths and masses of the samples collected using the three devices. The results showed that the BioPince collected the longest samples, and the Max-Core collected the shortest samples. It was expected that the Max-Core would

collect the shortest samples since the notch length was shorter than the throw lengths of the End-Cut needle biopsy devices; however, the average sample length was still shorter (by about 6 mm) than the notch length of the 1825 model. Two-tailed hypothesis tests were performed to test for statistical significance in the difference in the mean sample lengths of the three devices. Since the Max-Core's notch length was 15 mm shorter than the throw lengths of the other two devices, the hypothesis tests involving the Max-Core used sample length measurements that were normalized by dividing by the device's notch length (Max-Core) or throw length (BioPince and UF device). The null hypothesis for the test comparing the BioPince and the UF device was that the mean sample lengths were equivalent. The hypothesis tests comparing the Max-Core samples to those collected using the other two devices did not yield statistically significant differences in normalized mean sample lengths (p-values of 0.6317 and 0.7445 for comparisons with the BioPince and UF devices, respectively). The difference in average sample lengths of the BioPince and UF device were also not statistically significant (p-value of 0.1909).

The mass results showed that the UF device collected the most massive samples while the Max-Core samples had the least mass. It was expected that the Max-Core samples would have less mass since it is a Side-Cut needle, and its notch length is shorter than the throw lengths of the End-Cut devices. A two-sample two-sided hypothesis test was performed to analyze the statistical significance of the difference in the average sample masses collected by the BioPince and the UF device. The test resulted in a statistically significant difference (p-value of 0.0002). The finding that the

device that collected the longest samples (BioPince) did not also collect the samples with the most mass (UF device) potentially indicated a degree of tissue distortion. Either the BioPince was stretching its samples, or the UF device was compressing its samples.

There are several possible causes of tissue distortion. For the case of BioPince stretching the sample, the pincing mechanism may drag and stretch the sample as it cuts through the tissue. The high strain rate from the high-speed firing mechanism may also contribute to sample distortion. For the case of the UF device compressing the sample, one possibility is that the vacuum of the syringe is sucking additional tissue into the needle beyond the throw length. This suction of additional tissue could be compressing the tissue inside the needle. Although the failure mechanism that causes the sample to break away from the surrounding tissue is tensile in the case of the UF device, the potential for compression from the vacuum should not be ignored. Further testing is necessary to determine the extent and cause of sample tissue distortion mechanism for the BioPince and the UF device.

Furthermore, a unique ball-like structure was observed at the distal ends of some of the samples collected using the UF device, as shown in Fig. 11. The size of the ball-like structure (when present) also varied, as shown in the porcine liver and bovine cardiac tissue samples in Fig. 11(b) and Fig. 11(c). In contrast, a ball-like structure did not clearly appear in any of the samples collected using the other two commercial devices in the present study.

Formation of the ball-like structure was also observed while collecting the low-concentration-gelatin samples using the larger proof-of-concept device developed in the

previous study [14], upon which the UF device was modeled. This is believed to be caused by an end of the gelatin sample becoming trapped in the clearance between the inner stylette and the external needle (0.75-0.1 mm in radius) during biopsy. When the sample was extracted from the coaxial needle, the sample was relaxed and deformed, forming the ball-like structure at the distal end. In the previous study, the coaxial needles consisted of an external needle (1.27 mm OD and 1.14 mm ID) and inner stylette (0.94 or 0.99 mm in diameter) [14]. In the present study, the same external needle was used with a 0.94 mm diameter inner stylette.

The ball-like structure may be a useful feature in determining sample orientation and locating diseases found in patients since the feature only appears on the distal end of the samples. Although more studies in the ball-structure formation are needed, Fig. 11 shows that the UF device has this unique potential.

CONCLUSIONS AND FUTURE WORK

The conclusions drawn from this work can be summarized as follows:

1. A handheld aspiration-assisted biopsy device with an End-Cut coaxial needle (UF device) was developed and shown to perform comparably to two commercially available prostate needle biopsy devices (i.e. BioPince and Max-Core). The UF device enables the collection of more massive samples compared to the two commercially available devices.
2. The UF device is capable of collecting a wider range of tissue types (e.g. samples with low stiffness) compared to the two commercially available devices.

3. The samples collected by the UF device display a ball-like structure on the distal end of the samples, which may be useful in determining sample orientation within the body or organ.
4. Stiffness alone is not a sufficient indicator of phantom suitability, as was illustrated by the performance of the BioPince and Max-Core on the gelatin samples.

Significant sample distortion can interfere with sample analysis and the subsequent diagnosis. Therefore, future work will include identification of the sample-distortion mechanisms in the UF device and the proposal of methods to minimize the distortion. As mentioned above, the ball-like structure shown at the distal ends of the samples (see Fig. 11) has potential for tissue-orientation marking. However, the controllability of the structure is unknown. This is a topic that needs to be addressed to exploit the structure in the future.

The UF device was originally developed for prostate-cancer biopsy, but the device applications should not be limited to prostate-cancer diagnosis. Accordingly, it is essential that the vacuum of the proposed device is sufficient to collect higher-stiffness tissue samples. This may require a larger-diameter syringe or a variable needle-throw length to accommodate various applications. Programmability of the needle throw length may be a desired feature in the future.

ACKNOWLEDGMENT

The authors would also like to express their thanks to Keegan Bess and Kandice Ribeiro for their support for experimentation.

FUNDING

N/A

NOMENCLATURE

BPH	benign prostate hyperplasia
RTE	real-time tissue elastography
AFM	atomic force microscopy
SWE	shear wave elastography
MMP-2	matrix metalloproteinase-2
DC	direct current
PLA	polylactic acid
LED	light emitting diode
PTFE	Polytetrafluoroethylene
OD	outer diameter
ID	inner diameter

REFERENCES

[1] American Cancer Society, 2021, "Key statistics for prostate cancer: Prostate cancer facts." Accessed November 29, 2021. https://www.cancer.org/cancer/prostate-cancer/about/key-statistics.html. Accessed: 16-Sep-2024.

[2] Kelley Brantley, and Katie Sikora, 2021, "Earlier cancer detection improves quality of life and patient outcomes," *Avalere Health*, July 29, 2021. https://avalere.com/insights/earlier-cancer-detection-improves-quality-of-life-and-patient-outcomes. [Accessed: 16-Sep-2024].

[3] C. Schroeder, L. Loebelenz, J. Heverhagen, G. Noeldge, M. Onnimann, S. Kim, M. Brönnimann, 2020, "Full core technology versus notch sampling technology: evaluation of the diagnostic accuracy and the risk of a pneumothorax after transthoracic needle biopsy of suspicious lung lesions." Acta Radiologica, December 26, 2020, 63(1): 35-41. DOI: 10.1177/0284185120981575.

[4] Max-CoreTM Disposable Core Biopsy Instrument. Accessed September 16, 2024. https://www.bd.com/en-us/products-and-solutions/products/product-families/max-core-disposable-core-biopsy-instrument

[5] MagnumTM Reusable Core Biopsy Instrument. Accessed September 16, 2024. https://www.bd.com/en-us/products-and-solutions/products/product-families/magnum-reusable-core-biopsy-instrument

[6] MonoptyTM Disposable Core Biopsy Instrument. Accessed September 16, 2024. https://www.bd.com/en-ca/products-and-solutions/products/product-page.121820

[7] Temno Evolution® Biopsy Device - Four-Bevel Tip - Merit Medical. Accessed September 16, 2024. https://www.merit.com/peripheral-intervention/biopsy/soft-tissue-biopsy/temno-evolution-biopsy-device/

[8] CorVocetTM Biopsy System - Sleek Lines & Ergonomic Grip. Accessed September 16, 2024. https://www.merit.com/peripheral-intervention/biopsy/soft-tissue-biopsy/corvocet-biopsy-system/

[9] Achieve® Automatic Biopsy Device - Precise Control & Quality Sampling. Accessed September 16, 2024. https://www.merit.com/product/achieve-automatic-biopsy-device/

[10] BioPince Ultra® Full Core Biopsy Instrument. Accessed September 16, 2024. https://www.argonmedical.com/product/biopince-ultra-full-core-biopsy-instrument/

[11] SuperCoreTM Semi-Automatic Biopsy Instrument. Accessed September 16, 2024. https://www.argonmedical.com/products/supercore-semi-automatic-biopsy-instrument

[12] Tru-CoreTM II Automatic Biopsy Instrument. Accessed September 16, 2024. https://www.argonmedical.com/products/tru-core-ii-automatic-biopsy-instrument

[13] K. D. Hopper, C.S. Abendroth, K. W. Sturtz, Y. L. Matthews, J. S. Hartzel, and P. S. Potok, 1995, "CT percutaneous biopsy guns: comparison of end-cut and side-notch devices in cadaveric specimens." American Journal of Roentgenology, January 1995, 164(1): 195-199. DOI: 10.2214/ajr.164.1.7998539.

[14] P.-Y. Wu, H. Kahraman, and H. Yamaguchi, 2017, "Development of aspiration-assisted end-cut coaxial biopsy needles," ASME Journal of Medical Devices, March 2017; 11(1): 011012. DOI: 10.1115/1.4035688.

[15] E. C. Faria, N. Ma, E. Gazi, P. Gardner, M. Brown, N. W. Clarke, and R. D. Snook, 2008, "Measurement of elastic properties of prostate cancer cells using AFM," Analyst, July 25, 2008; 133(11): 1498-1500. DOI: 10.1039/B803355B.

[16] X. Wang, J. Wang, Y. Liu, H. Zong, X. Che, W. Zheng, F. Chen, Z. Zhu, D. Yang, and X. Song, 2014, "Alterations in mechanical properties are associated with prostate cancer progression," Medical Oncology, February 7 2014, 31(3): 876. DOI: 10.1007/s12032-014-0876-9.

[17] R. Cao, Z. Huang, T. Varghese, and G. Nabi, 2013, "Tissue mimicking materials for the detection of prostate cancer using shear wave elastography: A validation study," Medical Physics, February 2013, 40(2); 022903. DOI: 10.1118/1.4773315.

[18] S. Pheasant, C. M. Haslegrave, 1996, *Bodyspace: Anthropometry, Ergonomics And The Design Of Work*, CRC Press, UK.

[19] A. Mital, 1991, "Hand Tools: Injuries, Illnesses, Design, and Usage", in Workspace, Equipment and Tool Design, vol. 15, A. Mital and W. Karwowski, Eds. Elsevier, 1991, 219–256. DOI: 10.1016/B978-0-444-87441-2.50014-5.

511 **Figure Captions List**
512

513
514

515 **Table Caption List**
516

Table 1 Feature summary of on-the-market prostate biopsy devices

Table 2 Biopsy device features and conditions comparison

517

Table 1 Prostate biopsy devices

Brand	Name	Type of cut	Biopsy type	Needle		Sample length (mm)	Actuator
				Size (gauge)	Penetration depth (mm)		
Bard/BD	Max-Core [4]	Side cut	Core	14,16,18,20	22	18, 19	Spring/Disposable
Bard/BD	Magnum [5]	Side cut	Core	12,14,16,18,20	15, 22	-	Spring/Reusable
Bard/BD	Monopty [6]	Side cut	Core	12,14,16,18,20	11, 22	7, 17	Spring/Disposable
Merit Medical	Temno [7]	Side cut	Core	14,16,18,20	15, 28	10, 20	Spring/Disposable
Merit Medical	CorVocet [8]	End cut	Full core	14,16,18,20	17–27	15–25	Spring/Disposable
Merit Medical	Achieve [9]	Side cut	Core	14,16,18,20	25	20	Spring/Disposable
Argon Medical	BioPince [10]	End cut	Full core	16, 18	13, 23, 33	9, 19, 29	Spring/Disposable
Argon Medical	SuperCore [11]	Side cut	Core	14,16,18,20	12, 22	9.5, 19	Spring/Disposable
Argon Medical	Tru Core [12]	Side cut	Core	14,16,18,20	22	19	Spring/Disposable

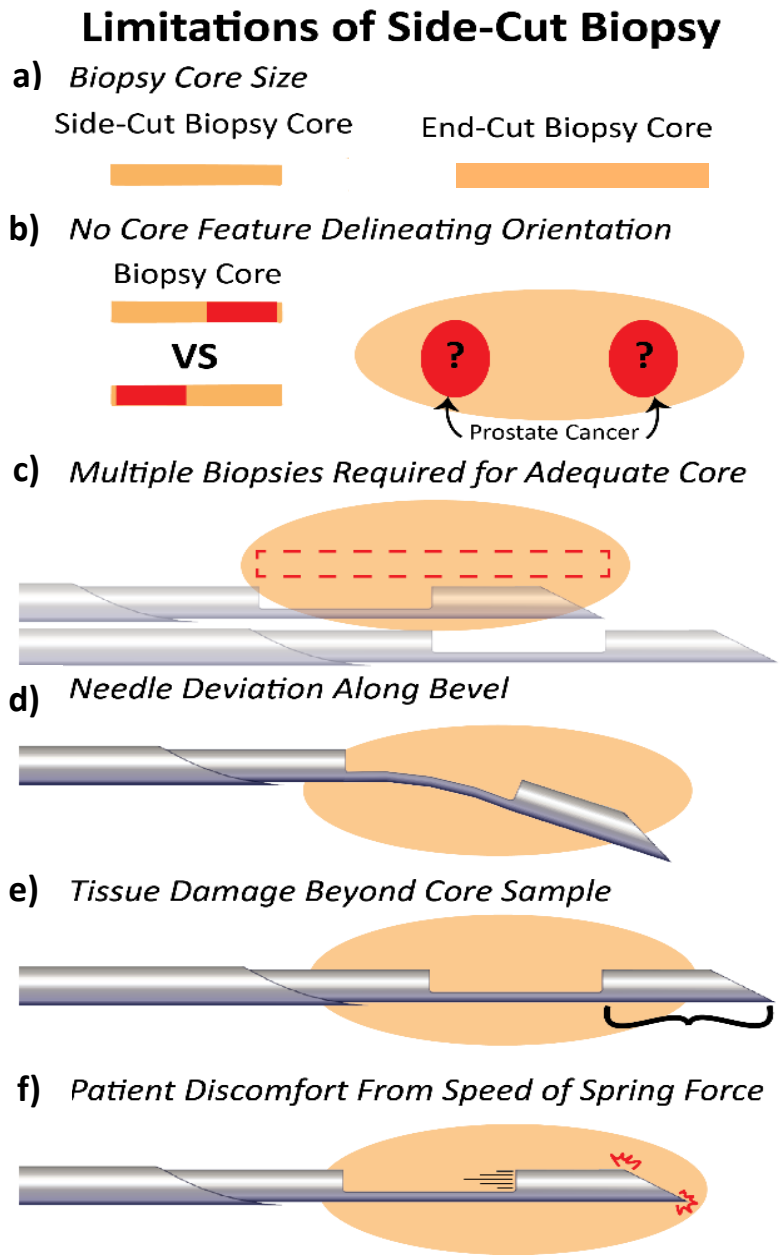
Limitations of Side-Cut Biopsy
a) Biopsy Core Size
Side-Cut Biopsy Core
End-Cut Biopsy Core
b) No Core Feature Delineating Orientation
Biopsy Core
VS
?
?
Prostate Cancer
c) Multiple Biopsies Required for Adequate Core
d) Needle Deviation Along Bevel
e) Tissue Damage Beyond Core Sample
f) Patient Discomfort From Speed of Spring Force

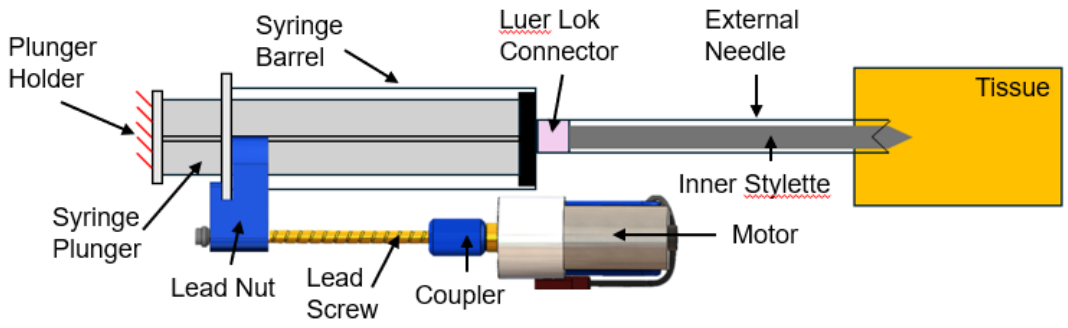

(a) Coaxial needle is inserted in tissue. Motor and Plunger Holder are fixed to the housing.

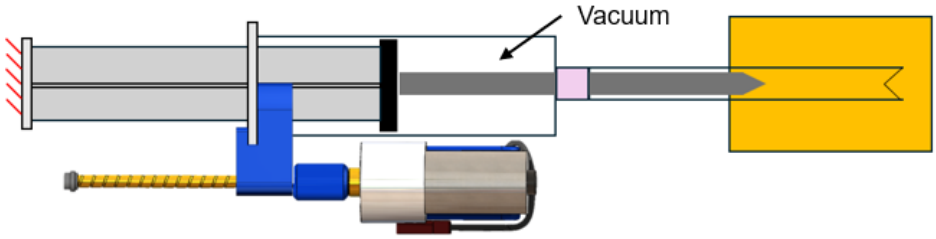

(b) Motor is activated and moves syringe barrel forward until jams, which causes the motor current to spike to the stall current value. This current spike is detected by a current sensor in the controller.

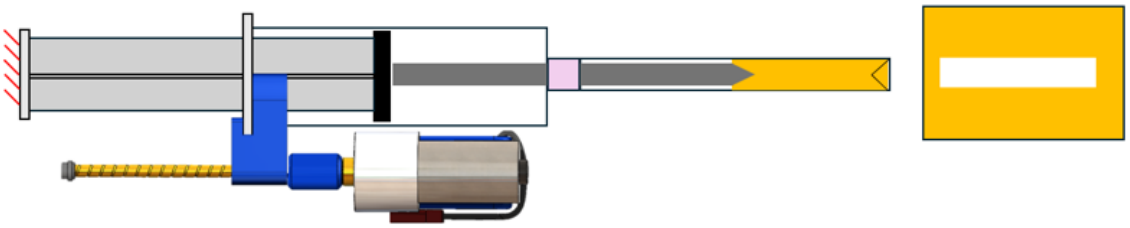

(c) Device is retracted from tissue. Tissue is held inside the needle by the vacuum, and the sample breaks away from the tissue .

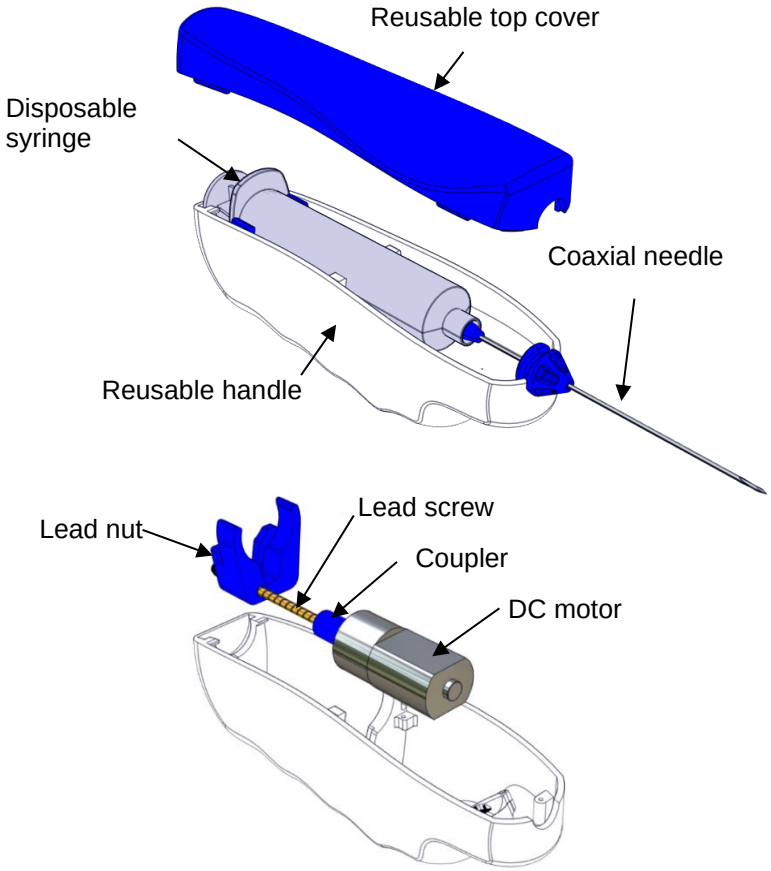
Reusable top cover
Disposable syringe
Coaxial needle
Reusable handle
Lead nut
Lead screw
Coupler
DC motor

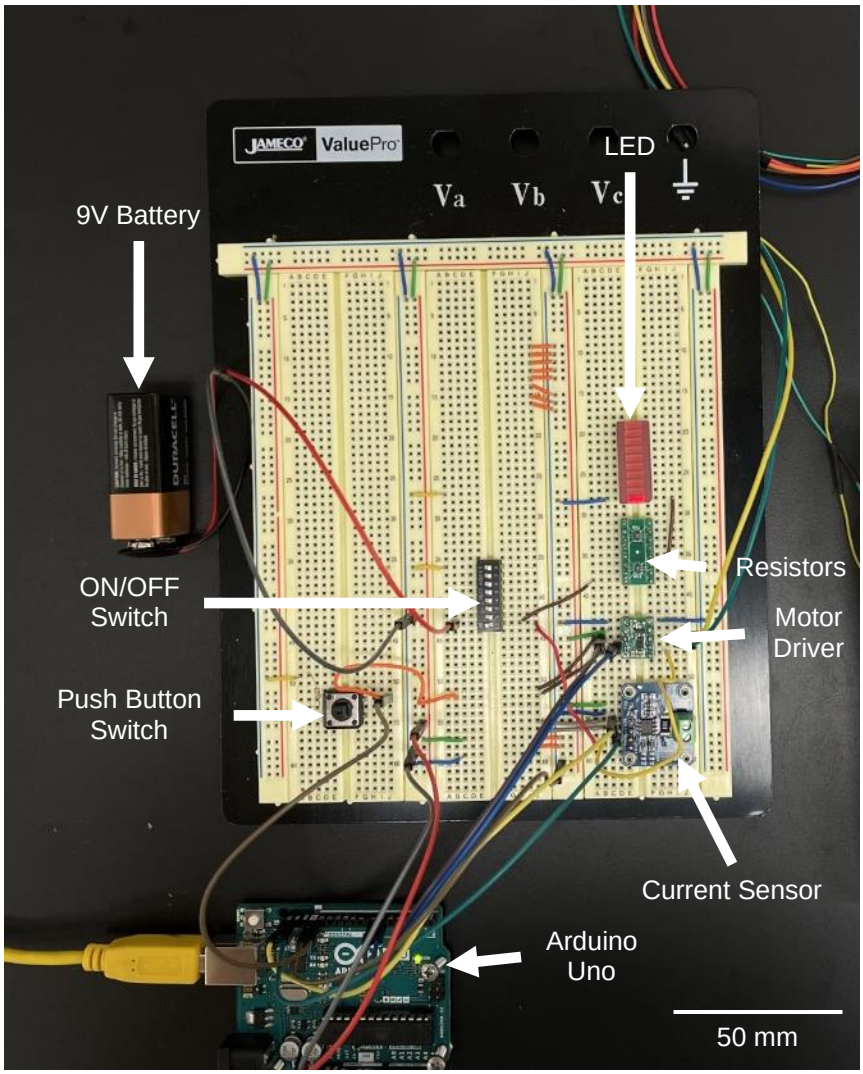
JAMECO ValuePro
Va
Vb
Vc
LED
9V Battery
ON/OFF Switch
Push Button Switch
Resistors
Motor Driver
Current Sensor
Arduino Uno
50 mm

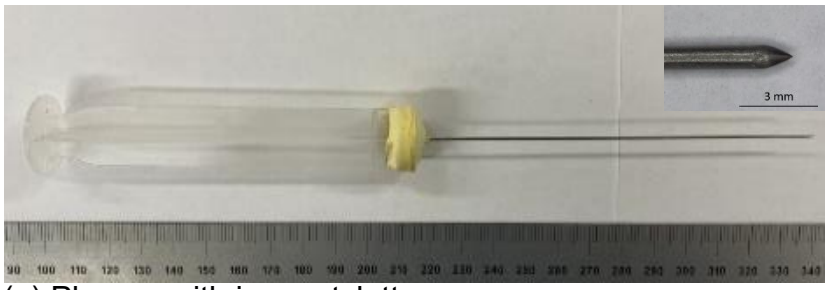

(a) Plunger with inner stylette

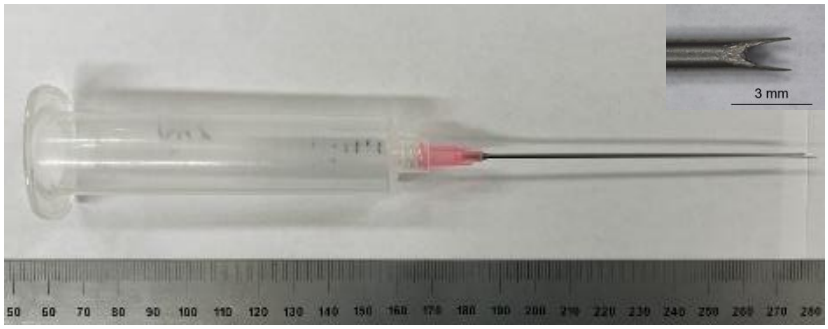

(b) Barrel with external needle

(c) Full syringe and needle assembly

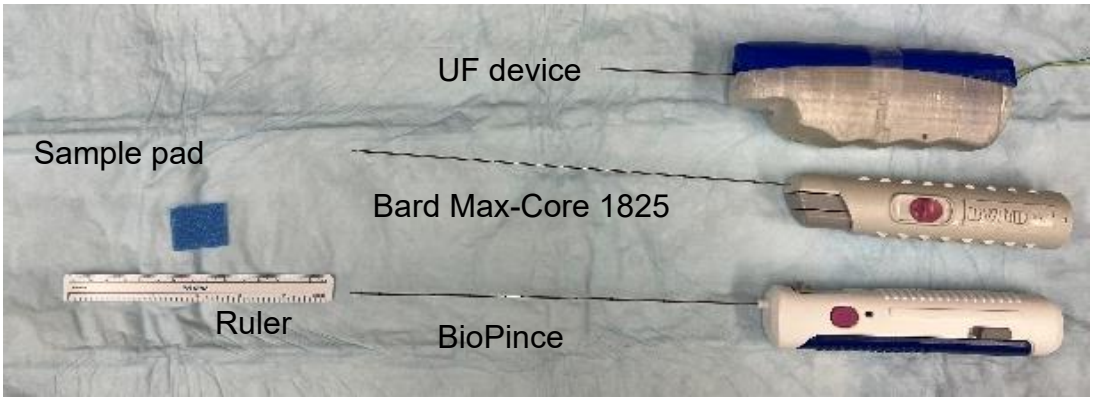
UF device
Sample pad
Bard Max-Core 1825
Ruler
BioPince

Table 2 Experimental conditions

Device	Bard 1825	BioPince	UF device
Needle	18G Side-Cut needle	18G End-Cut needle	18G End-Cut needle
Throw length	25 mm	33 mm	23, 33 mm
Needle length	275 mm	265 mm	100 mm
Needle driving mechanism	Spring-Loaded Firing		DC motor + lead screw

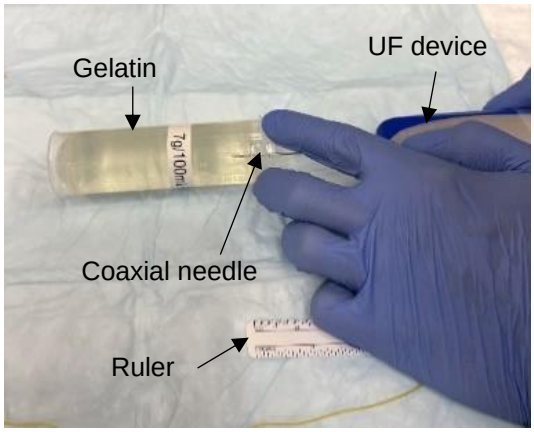

(a) Needle insertion into gelatin specimen

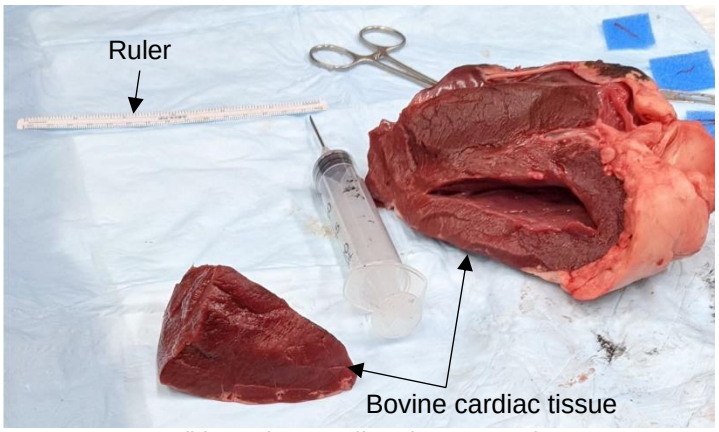

(b) Bovine cardiac tissue *ex-vivo*

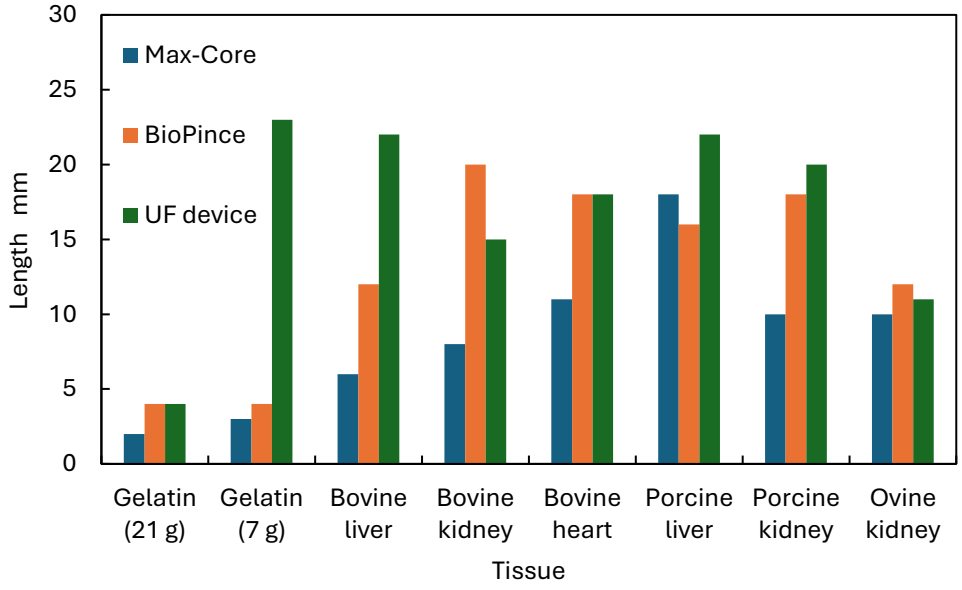

(a) Sample lengths

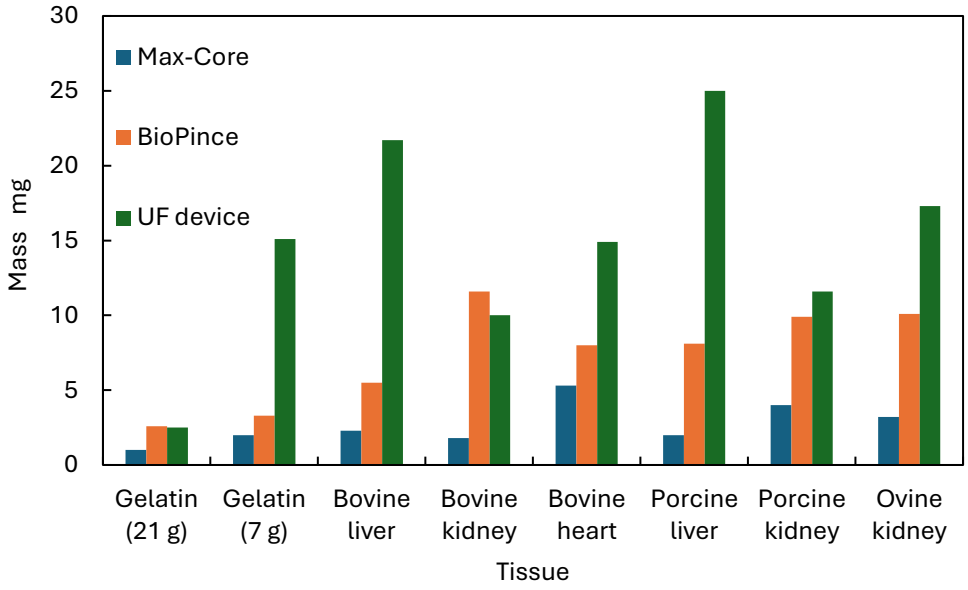

(b) Sample masses

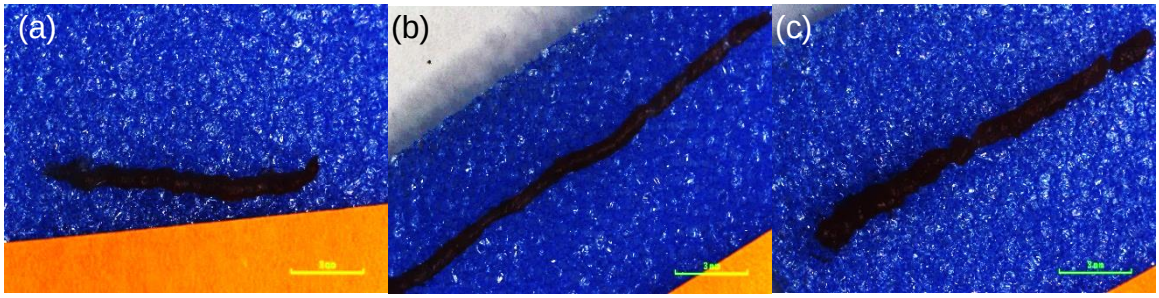
(a)
(b)
(c)

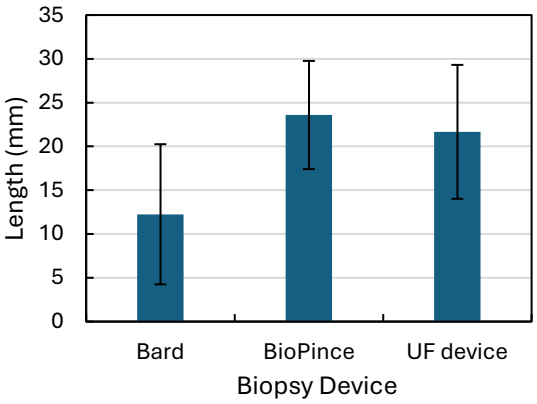

(a) average sample lengths

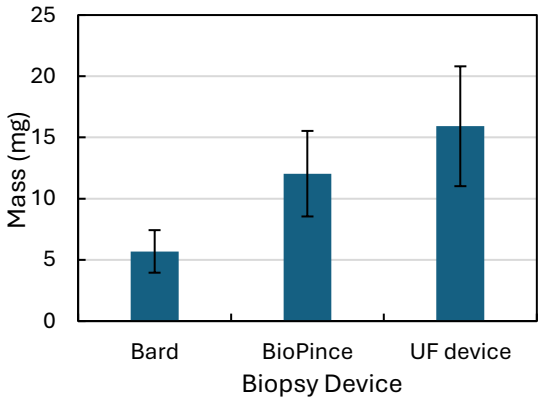

(b) average sample masses

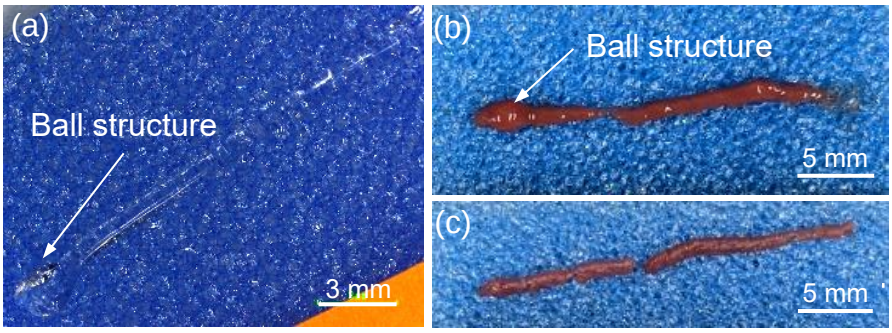
(a)
Ball structure
3 mm
(b)
Ball structure
5 mm
(c)
5 mm